Journal of Environmental Chemical Engineering 12 (2024) 111469

Contents lists available at ScienceDirect

Journal of Environmental Chemical Engineering

journal homepage: www.elsevier.com/locate/jece

Thermally activated natural chalcopyrite for Fenton-like degradation of Rhodamine B: Catalyst characterization, performance evaluation, and catalytic mechanism

Jiapeng Yang [a,d], Kai Jia [a,b,c,*], Shaoyong Lu [d], Yijun Cao [a,b,c], Grzegorz Boczkaj [e,f,**], Chongqing Wang [a,b,*]

[a] School of Chemical Engineering, Zhengzhou University, Zhengzhou 450001, China
[b] The Key Lab of Critical Metals Minerals Supernormal Enrichment and Extraction, Ministry of Education, Zhengzhou 450001, China
[c] Zhongyuan Critical Metal Laboratory, Zhengzhou University, Zhengzhou, Henan 450001, China
[d] National Engineering Laboratory for Lake Pollution Control and Ecological Restoration, Research Centre of Lake Environment, Chinese Research Academy of Environmental Sciences, Beijing 100012, China
[e] Gdańsk University of Technology, Faculty of Civil and Environmental Engineering, Department of Sanitary Engineering, G. Narutowicza St. 11/12, 80-233 Gdansk, Poland
[f] EkoTech Center, Gdansk University of Technology, G. Narutowicza St. 11/12, 80-233 Gdansk, Poland

ARTICLE INFO

miscellaneous: Editor: Luigi Rizzo

Keywords:
Degradation
Chalcopyrite
Rhodamine B
Wastewater treatment
Fenton process

ABSTRACT

In this work, catalytic activity of natural chalcopyrite ($CuFeS_2$) was improved by thermal activation. The modified chalcopyrite was used as efficient catalyst for degradation of organic dye Rhodamine B (RhB) through advanced oxidation process (AOP). Effects of catalyst dosage, H_2O_2 concentration, reaction temperature, solution pH, anions, and natural organic matter on the degradation efficiency of RhB were investigated. This study revealed that thermal activation at 300 °C changed the chemical valency of surface elements rather than transforming the major chemical phase of natural chalcopyrite. The Fenton-like degradation of RhB was significantly improved by thermally activated chalcopyrite. RhB degradation could be obtained under broad pH and showed high resistance to natural organic matter and anions. Under optimal conditions of H_2O_2 43.0 mM, catalyst 0.75 g/L, initial pH 5.1, and reaction temperature 25 °C, the degradation of RhB reached 96.7% at 50 min. Based on the rate constant of reaction kinetics, the activation energy for RhB degradation was calculated to be 9 kJ/mol. Radical scavenging experiments and electron paramagnetic resonance (EPR) technique demonstrated that RhB degradation was dominated by the generated hydroxyl radicals in activated chalcopyrite/H_2O_2 system. The formation of surface sulfates resulted from thermal activation induced the dissolved copper or iron ions, and promoted H_2O_2 activation and facilitated RhB degradation by reactive hydroxyl radicals. This work provides an in-depth understanding of the mechanism behind thermal activation to enhance the activity of natural chalcopyrite, offering a theoretical basis for utilizing natural minerals for Fenton-like treatment of organic wastewater towards cleaner production.

1. Introduction

In recent decades, with the accelerated industrialization of society, the discharge of organic wastewater significantly increases and causes serious threats to public health and eco-environment [26,35,66]. Organic wastewater contains a large number of toxic, harmful, and persistent organic pollutants, such as dyes, phenols, antibiotics, polychlorinated biphenyls, aromatic amines, and petroleum pollutants [28,5,61]. These organic pollutants are discharged into the environment with wastewater, and are likely to accumulate in the aquatic environment, which will affect the transfer mechanism of oxygen molecules and weaken the self-purification capacity of the aquatic environment,

* Corresponding authors at: School of Chemical Engineering, Zhengzhou University, Zhengzhou 450001, China
** Corresponding author at: Gdańsk University of Technology, Faculty of Civil and Environmental Engineering, Department of Sanitary Engineering, G. Narutowicza St. 11/12, 80-233 Gdansk, Poland.
E-mail addresses: jiakai@zzu.edu.cn (K. Jia), grzegorz.boczkaj@pg.edu.pl (G. Boczkaj), zilangwang@126.com (C. Wang).

https://doi.org/10.1016/j.jece.2023.111469
Received 12 September 2023; Received in revised form 17 October 2023; Accepted 9 November 2023
Available online 10 November 2023

leading to water pollution [69].

Advanced oxidation processes (AOPs) have been shown to be an efficient method for treating organic pollutants in wastewater [37,57,77]. AOPs produce strongly oxidizing ·OH with an oxidation potential of 2.80 V, and its oxidation capacity far exceeds that of common chemical oxidants (permanganate, H_2O_2, and O_3), and it can non-selectively degrade most organic pollutants [6]. For example, ·OH can effectively decompose the conjugated double bonds of dye chromophores as well as other groups, and the subsequent formation of smaller non-chromophore molecules reduces the color of the dye effluent [1]. Fenton process is one of common AOPs that rapidly and non-selectively degrades most organic pollutants and even mineralize them into CO_2 and H_2O [18]. In view of the limitations of the conventional Fenton process, such as strict reaction conditions, subsequent treatment of iron-containing sludge, and difficulty in recovering the catalyst, the heterogeneous Fenton or Fenton-like processes have attracted widespread attention [8,58]. The use of solid catalysts extends the pH range of the reaction, reduces the production of iron sludge, and favors the recovery of catalysts [34,62,70].

Various iron-based materials have been studied for Fenton-like degradation of organic pollutants, and most of them are well-designed and chemically synthesized. Complex synthesis process and high cost of used chemical reagents limit their potential application. Recently, researchers have turned their attention to natural iron-containing minerals [38]. The minerals are more readily available and cheaper than synthetic iron-based materials, and exhibit good catalytic activity in peroxide activation due to their unique components and crystallinity [23]. Sun et al. found the good degradation of sodium sulfadiazine under broad pH in the system of siderite/H_2O_2 [47]. Zhang and coworkers reported the efficient degradation of carmine with degradation efficiency of 99.97% in siderite/H_2O_2 system [71]. Studies have proven the feasibility of catalytic degradation of organic pollutants using natural minerals as catalysts, but the catalytic activity of natural minerals is commonly low. The catalytic activity of natural minerals can be enhanced by utilizing external energy. Pyrite has a narrow band gap (0.95 eV) and exhibits strong light absorption, which can be photo-activated to produce photoelectrons (e^-) and holes (h^+) [20,72]. When pyrite was utilized in the photo-Fenton system, the Fe^{3+}/Fe^{2+} cycle was significantly improved and the complete oxidation time of p-nitrophenol was reduced from 10 min to 4 min [76]. The introduction of an electric field in the AOP enhanced the oxidizing ability [38]. In addition to external physical fields, the degradation efficiency of natural minerals can be improved by adding reducing agents. Wang and colleagues demonstrated that the addition of hydroxylamine resulted in a more efficient degradation of acid orange 7 (55.5%) compared to the copper tailings/peroxydisulfate system (7.68%) [60]. Currently, catalytic degradation of organic pollutants using natural minerals is still poorly investigated, and strategies of improving catalytic activity of natural minerals are imperative.

Chalcopyrite ($CuFeS_2$) is a typical bimetallic iron sulphide mineral with potential for Fenton-like catalysis due to its efficient electron transfer properties [39,75]. In Li's study, the synthesized $CuFeS_2$ effectively activated sodium percarbonate to induce effective degradation of sulfadiazine (86.4%) under neutral conditions [29]. Since natural minerals are accompanied by impurities, the fragility, oxidation and stoichiometric ratio between unsaturated elements, the catalytic activity of natural chalcopyrite is detrimental [27]. In the previous work, natural chalcopyrite was proved to be potential heterogeneous catalyst for degradation of organic pollutants in H_2O_2-based AOP and persulfate-based AOP [67,75]. Mechanical activation induced the increase of surface area and surface oxidation of natural chalcopyrite, which improved its catalytic activity [59]. In this work, an innovation thermal activation was proposed to improve the catalytic activity of natural chalcopyrite. The objectives of this studies are to (i) examine the thermal activation of natural chalcopyrite by multiple characterizations; (ii) evaluate the catalytic performance for the degradation of target pollutant; (iii) understand the catalytic mechanism of Fenton-like reactions.

2. Materials and methods

2.1. Materials

The natural chalcopyrite used in this work was obtained from Dongchuan copper mine in Yunnan Province, China. The grade of $CuFeS_2$ and Cu in the natural chalcopyrite was 90.3–92.1% and 31.2–31.9%, respectively. All chemicals used in this work were analytically pure and used as received without further purification. Hydrogen peroxide (H_2O_2, 30%), isopropyl alcohol (C_3H_8O; IPA), and tert-butanol ($C_4H_{10}O$; TBA), were obtained from Shanghai Aladdin Bio-Chem Technology Co., LTD (China). Rhodamine B ($C_{28}H_{31}ClN_2O_3$, RhB) was purchased from Tianjin Dehua Chemical Reagent Factory. Ultrapure water (18.25 MΩ·cm) was used in all experiments.

2.2. Thermal activation of natural chalcopyrite

The sample of natural chalcopyrite was smashed and manually ground, passed through a 200-mesh sieve, and the sieved powder was collected. A 10 g of the powder was placed in a crucible and located in a muffle furnace, and the temperature was heated to specific value at a rate of 5 ℃/min and treated for 2 h under air atmosphere. Preliminary experiments were conducted to examine the effect of the temperature (100, 200, 300, and 400 °C) of thermal activation, and 300 °C was selected as optimized temperature for thermal activation of natural chalcopyrite. The thermally activated chalcopyrite was used as catalyst for Fenton-like degradation of RhB.

2.3. Characterizations

Morphology was examined using a FEI Quanta FEG 250 scanning electron microscope (SEM, USA), and elemental distribution was determined by energy dispersive spectroscopy (EDS). N_2 adsorption/desorption isotherm was conducted using a Micromeritics ASAP 2020 surface area analyzer (USA), and Brunauer-Emmett-Teller method and Barret-Joyner-Halenda method were used to calculate the surface area and pore size, respectively. A Rigaku Ultimate IV X-ray diffraction spectrometer (XRD, Japan) was used to analyze chemical phases and crystal structures. Surface elemental valence changes were detected by Thermo ESCALAB 250XI X-ray photoelectron spectroscopy (XPS, USA). The leached metal ions during the reaction were determined using an Avio 500 PerkinElmer inductively coupled plasma-optical emission spectrometer (ICP-OES; USA). Electron paramagnetic resonance (EPR) signals were measured by a JES FA200 spectrometer (JEOL, Japan) using 5,5-Dimethyl-1-pyrroline-N-oxide (DMPO) as trapping agent to identify hydroxyl radical. The concentration of RhB was measured spectrophotometrically with a detection wavelength of 554 nm using a Shimadzu UV-2600 spectrometer (Japan).

2.4. Degradation experiments

Degradation experiments were carried out in 150 mL conical flasks placed in a thermostatic oscillator and shaken at 150 rpm. The thermally activated chalcopyrite and H_2O_2 were added into RhB solution to initiate catalytic degradation reaction. The effects of H_2O_2 concentration, catalyst dosage, initial pH, anions, natural organic matter, and temperature on RhB degradation were studied. The initial pH of RhB solution was adjusted to specific value (3.0, 4.0, 5.1, 7.0, 9.0, and 11.0) using HCl or NaOH solution. The solution samples were taken out at regular time intervals, centrifuged for 1 min, and measured the absorbance of the solution by UV-Vis spectroscopy. The mean values of degradation experiments were given in this work. The degradation (%) of RhB was calculated by Eq. (S1). The reaction kinetics were examined

using a pseudo-first-order model (Eq. (S2)), and the activation energy was calculated according to the Arrhenius equation (Eq. (S3)).

3. Results and discussion

3.1. Characterizations of thermally activated chalcopyrite

The phase composition of natural chalcopyrite before and after thermal activation were examined by XRD analysis. As shown in Fig. 1a, the characteristic peaks of $CuFeS_2$ at $2\theta = 29.4°$, 33.9°, 48.7°, 49.1°, 57.9°, 58.6°, 71.3°, 78.9°, and 79.6° are observed in XRD pattern of natural chalcopyrite, corresponding to the (1 1 2), (2 0 0), (2 2 0), (2 0 4), (3 1 2), (1 1 6), (4 0 0), (3 3 2), and (3 1 6) planes of $CuFeS_2$ (PDF #37–0417), respectively [15]. The intensity of the characteristic peaks of chalcopyrite increases significantly and becomes sharper after thermal activation, indicating an increase in the crystallinity of chalcopyrite [17]. The position of the characteristic peaks does not shift before and after thermal activation, and no new peaks appear, indicating that no other phases of chalcopyrite form after thermal activation of natural chalcopyrite.

The pore structure and surface area of chalcopyrite are characterized by N_2 adsorption/desorption isotherms (Fig. 1b). Chalcopyrite before and after thermal activation is characterized by type IV isotherm [67]. The specific surface area and pore volume are listed in Table S1. The specific surface area of natural chalcopyrite before and after thermal activation is 0.989 and 1.037 m^2/g, while the pore volume and pore size decrease slightly. The results are similar to the surface area and pore size of $CuFeS_2$ reported by Rupa Ranjani et al. [44] Thus, thermal activation does not change the surface area and pore size of chalcopyrite.

The SEM images shown in Fig. 2 illustrate the morphology of chalcopyrite before and after thermal activation. The particle size of natural chalcopyrite is relatively large, and shows smooth surface without porous structure. Thermal activation does not significantly change the surface of natural chalcopyrite, and the surface becomes slightly wrinkled and fragmented. This can be ascribed to the surface oxidation of iron sulphide minerals during thermal activation in air atmosphere [49]. EDS analysis reveals that the main elements in natural chalcopyrite are iron (36.7%), copper (35.1%), and sulfur (25.1%). The content of the copper and iron in thermally activated chalcopyrite significantly decreases, while the content of oxygen increases, indicating that the surface of chalcopyrite can be oxidized during the thermal activation [49].

The XPS spectra of chalcopyrite before and after thermal activation are shown in Fig. S1. The presence of Fe 2p, Cu 2p, S 2p, and O 1 s is verified by the characteristic peaks at the binding energies of 713.1 eV, 932.1 eV, 162.1 eV, and 533.1 eV, respectively [33]. The significant enhancement of the intensity of O 1 s peak after thermal activation suggests the potential surface oxidation of chalcopyrite. The high-resolution Cu 2p spectra are represented in Fig. 3a. For the natural chalcopyrite, the two peaks at the binding energies of 932.1 eV and 952.1 eV correspond to Cu 2p3/2 and Cu 2p1/2, demonstrating the presence of Cu^+ and Cu^{2+} in natural chalcopyrite [43]. For thermally activated chalcopyrite, the peaks assigned to Cu^+ and Cu^{2+} are not significantly changed, indicating minor Cu oxidation on the surface of chalcopyrite. The high-resolution spectra of Fe 2p of chalcopyrite are represented in Fig. 3b. The peaks at 707.7 eV, 711.3 eV, and 721.7 are attributed to Fe^{2+}, while the peaks at 712.8 eV and 725.8 are assigned to Fe^{3+} [54]. After thermal activation, the Fe 2p3/2 peaks shift to higher binding energies, demonstrating the oxidation of iron on the surface of the chalcopyrite. The peaks at about 710–718 eV prove the presence of iron oxides (e.g., Fe_2O_3 at about 710.69 eV) [10] and sulfates (e.g., $FeSO_4$ at about 713.1 eV) [22]. In addition, the significant enhancement of the Fe 2p1/2 peak at 724.8 eV after thermal activation is related to the content of iron sulphate [11]. The high-resolution spectra of S 2p of chalcopyrite before and after thermal treatment are shown in Fig. 3c. The four peaks at 161.5 eV, 162.7 eV, 163.6 eV, and 169.2 eV are attributed to S^{2-}, S_2^{2-}, S_n^{2-}, and SO_4^{2-} of natural chalcopyrite surface. After thermal activation, the intensity of the S^{2-}, S_2^{2-}, and S_n^{2-} peaks is significantly reduced, and new peaks at 168.3 eV and 169.5 eV attributed to the sulphate species (SO_4^{2-}) can be observed after thermal activation [21]. Fig. 3d depicts the high-resolution spectra of O 1 s of chalcopyrite before and after thermal treatment. The peaks at 529.7 eV and 531.3 eV correspond to metal oxide and sulphate species, and the intensity of the characteristic sulphate peaks is enhanced after the thermal activation. This further confirms that sulphate is formed on the surface of chalcopyrite during the thermal activation. In summary, XPS analysis verifies that thermal activation changes the chemical valence of Cu, Fe and S species and induces surface oxidation of natural chalcopyrite.

3.2. Comparison of RhB removal in different systems

RhB is chosen as the target organic pollutant to evaluate the catalytic performance of the thermally activated chalcopyrite. Currently, dyes related pollutant gained high attention in the field of AOP based wastewater treatment [3,40,41]. Fig. S2 shows the comparison of RhB removal in different systems. In the presence of H_2O_2 and chalcopyrite alone, 6.7% and 3.7% of RhB is removed within 50 min, suggesting the limited contribution of H_2O_2 oxidation and adsorption by chalcopyrite to RhB removal. RhB degradation in thermally activated chalcopyrite/H_2O_2 system reaches 96.7% at 50 min. The rate constant of first-order kinetics is 0.2000 min^{-1}, remarkably higher than that for H_2O_2 (0.0080 min^{-1}) and chalcopyrite (0.0091 min^{-1}) alone. Therefore, the thermally activated chalcopyrite is effective for Fenton-like degradation of RhB degradation.

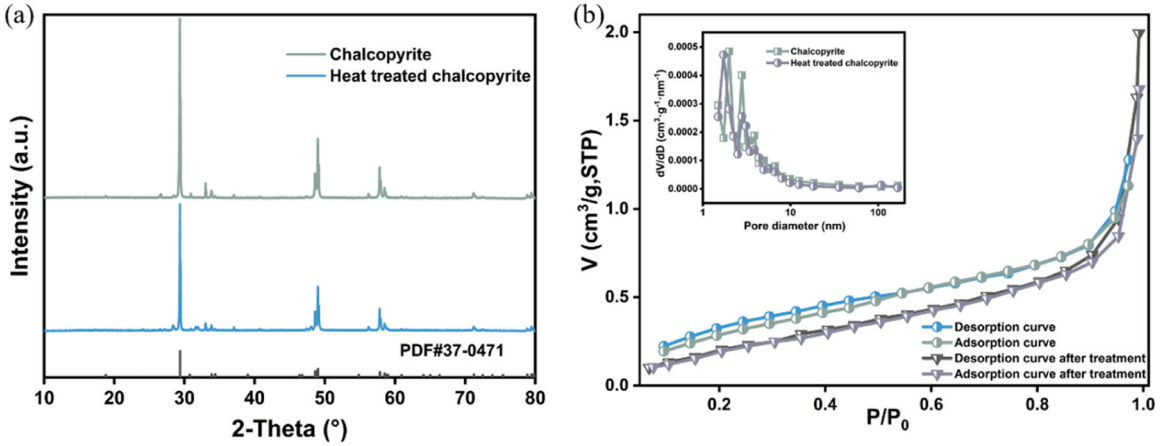

Fig. 1. (a) XRD spectra and (b) N_2 adsorption and desorption isotherms of chalcopyrite before and after thermal activation.

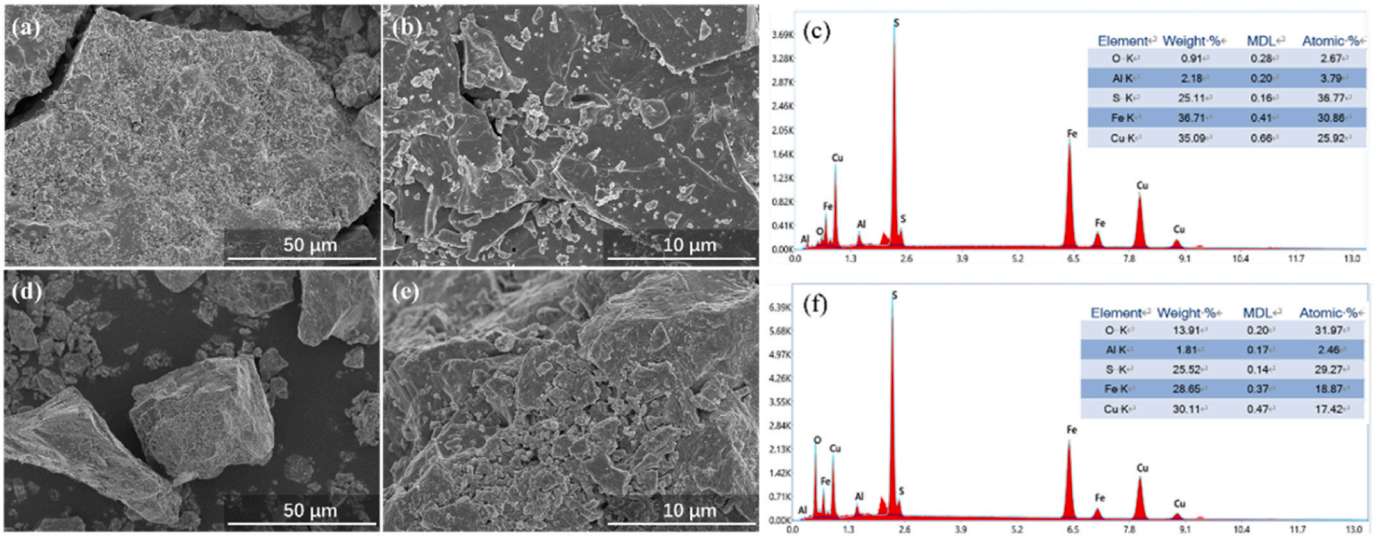

Fig. 2. (a, b) SEM images of chalcopyrite and (c) elemental content of natural chalcopyrite, (d, e) SEM images of chalcopyrite and (f) elemental content of chalcopyrite after thermal activation.

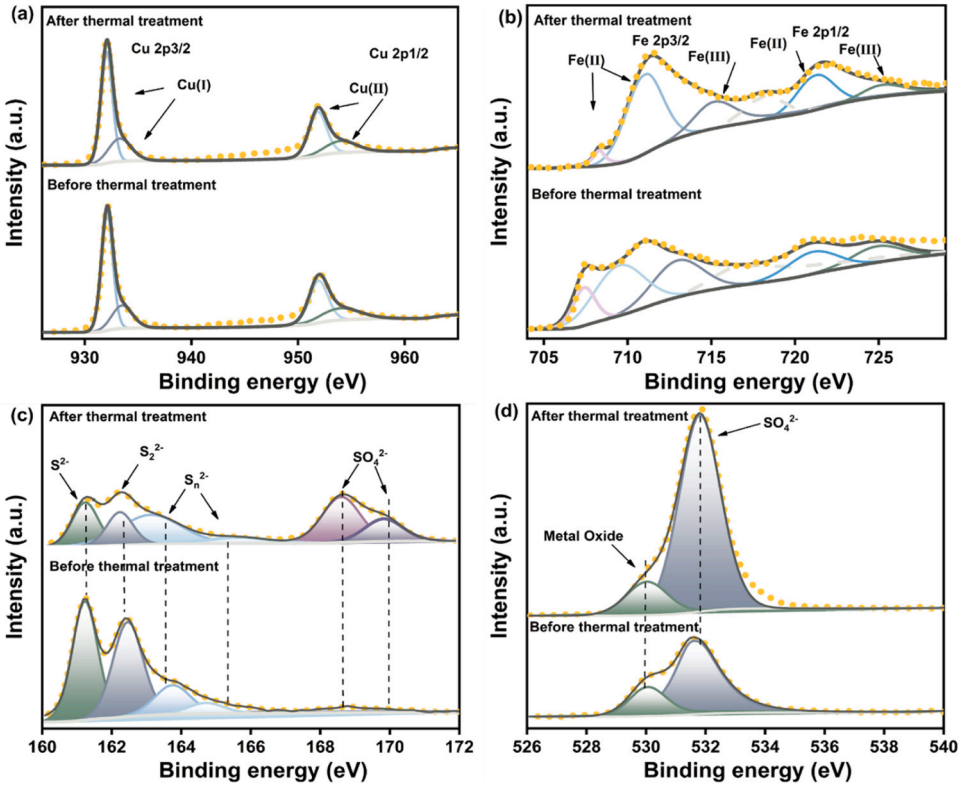

Fig. 3. High-resolution XPS spectra of chalcopyrite before and after thermal activation: (a) Cu 2p, (b) Fe 2p, (c) S 2p, (d) O 1 s.

3.3. *Effect of H_2O_2 concentration*

In the reaction system, the concentration of the oxidant H_2O_2 determines the amount of hydroxyl radical (·OH) produced [50]. Fig. 4a shows the effect of H_2O_2 concentration (0, 0.4, 21.5, 43.0 and 64.5 mM) on RhB degradation. The degradation of RhB is only 3.7% in absence of H_2O_2. As H_2O_2 concentration increases from 21.5 to 64.5 mM, the RhB degradation at 50 min increases from 79.7% to 97.2%. The production of •OH in solution can be increased by increasing H_2O_2 concentration in the Fenton-like system, thus promoting RhB degradation [31]. Fig. 4b exhibits that the rate constant increases from 0.0081 min^{-1} to 0.2236 min^{-1} as the concentration of H_2O_2 increases. When H_2O_2 concentration increases from 43.0 mM to 64.5 mM, the degradation efficiency of RhB does not change significantly, which is attributed to the scavenging effect of excess H_2O_2, producing HO_2• and •O_2^- with much lower oxidation potentials than •OH (Eqs. (1) and (2)) [52].

$$\bullet OH + H_2O_2 \rightarrow HO_2\bullet + H_2O \quad (1)$$

$$HO_2\bullet \rightarrow \bullet O_2^- + H^+ \quad (2)$$

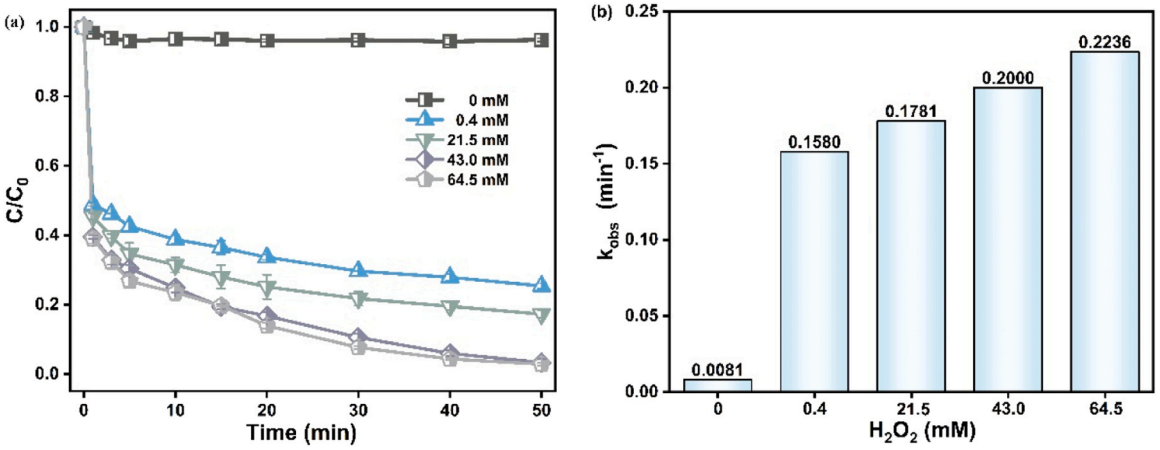

Fig. 4. (a) Effect of H_2O_2 concentration on RhB degradation, (b) rate constant at different H_2O_2 concentrations. Reaction conditions: chalcopyrite 0.75 g/L, pH 5.1, RhB 10 mg/L, and temperature 25 ℃.

3.4. Effect of catalyst dosage

Solid catalysts are essential in Fenton-like process, promoting the generation of reactive radical species for pollutant degradation [73]. The effect of chalcopyrite (0, 0.25, 0.50, 0.75 and 1.00 g/L) on RhB degradation is shown in Fig. 5a. The degradation of RhB is significantly increased by adding chalcopyrite from 0 g/L to 1.00 g/L. The degradation of RhB at 50 min gradually increases from 6.7% to 97.8%. Since the adsorption of RhB onto chalcopyrite is negligible, RhB removal is mainly due to the reaction of H_2O_2 with chalcopyrite to generate reactive radicals. The degradation efficiency of RhB at 50 min is 96.7% in the presence of 0.75 g/L chalcopyrite. However, there is no significant change in the degradation efficiency when catalyst increases from 0.75 g/L to 1.00 g/L, suggesting the saturation between the active site and H_2O_2 [16]. In Fig. 5b, the rate constant for RhB degradation increases from 0.0091 to 0.3309 min^{-1} by increasing chalcopyrite from 0.75 g/L to 1.00 g/L. The result can be attributed to the availability of more active sites on the catalyst surface and dissolved metal ions, which is beneficial to increase the reaction rate [29]. Since the excess chalcopyrite may cause the loss of reactive oxygen species and the leaching of metal ions [63], 0.75 g/L chalcopyrite is selected for subsequent experiments. Table S2 compares the degradation of RhB by different catalysts. The degradation of RhB by thermally activated chalcopyrite is comparable to or higher than that of previously reported catalysts such as natural chalcopyrite [67], pyrite [13], Fe@BC [56], $CoFe_2O_4$ @PPy [12], w-PCB [51]. Consequently, thermally activated chalcopyrite can efficiently activate H_2O_2 to achieve RhB degradation.

3.5. Effect of reaction temperature

The effect of reaction temperature (25, 30, 35, 40, and 45 °C) on RhB degradation is studied in the catalytic system. As shown in Fig. 6a, increasing the reaction temperature from 25 °C to 45 °C results in a slight increase in the degradation of RhB, and the degradation efficiency at 10 min is 72.5%, 75.1%, 77.1%, 81.9%, and 83.3%, respectively. The rate constant increases slightly from 0.1971 min^{-1} to 0.2409 min^{-1} (Fig. 6b). The positive correlation between RhB degradation and temperature is attributed to the fact that the increase in temperature accelerates the decomposition of RhB and promotes the production of ·OH [51]. In thermally activated chalcopyrite/H_2O_2 system, desirable RhB degradation can be achieved under ambient conditions. The activation energy for the degradation of RhB in the thermally activated chalcopyrite/H_2O_2 system is calculated from the Arrhenius equation to be 9 kJ/mol. The activation energy of RhB degradation for thermally activated chalcopyrite based AOP system is much lower than that of other previously reported catalysts, such as 40 kJ/mol for $CuCo_2S_4$ [65] or 69 kJ/mol for Fe_2O_3 [24]. The lower activation energy indicates that thermally activated chalcopyrite is promising for Fenton-like degradation of RhB.

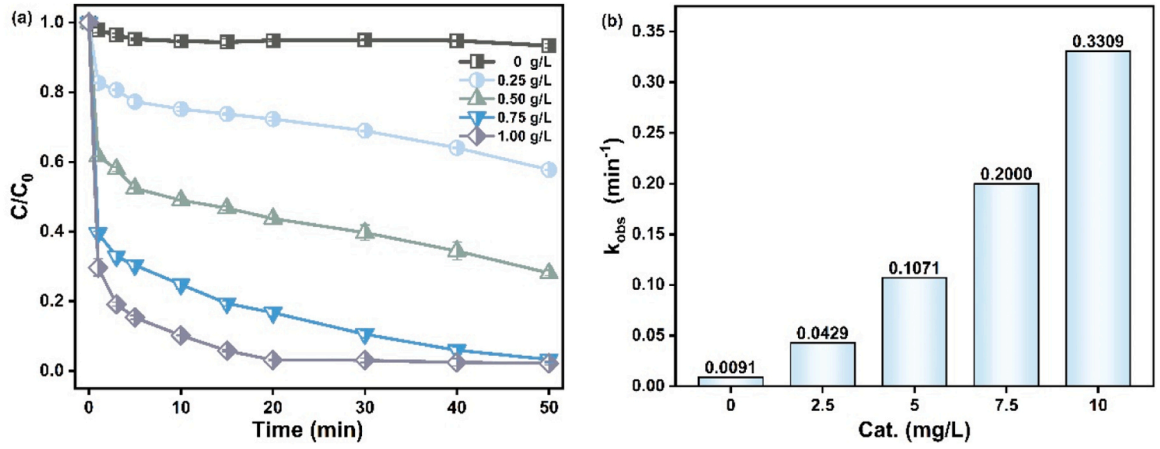

Fig. 5. (a) Effect of catalyst dosage on RhB degradation, (b) rate constant for different catalyst dosages. Reaction conditions: H_2O_2 43.0 mM, pH 5.1, RhB 10 mg/L, and temperature 25 ℃.

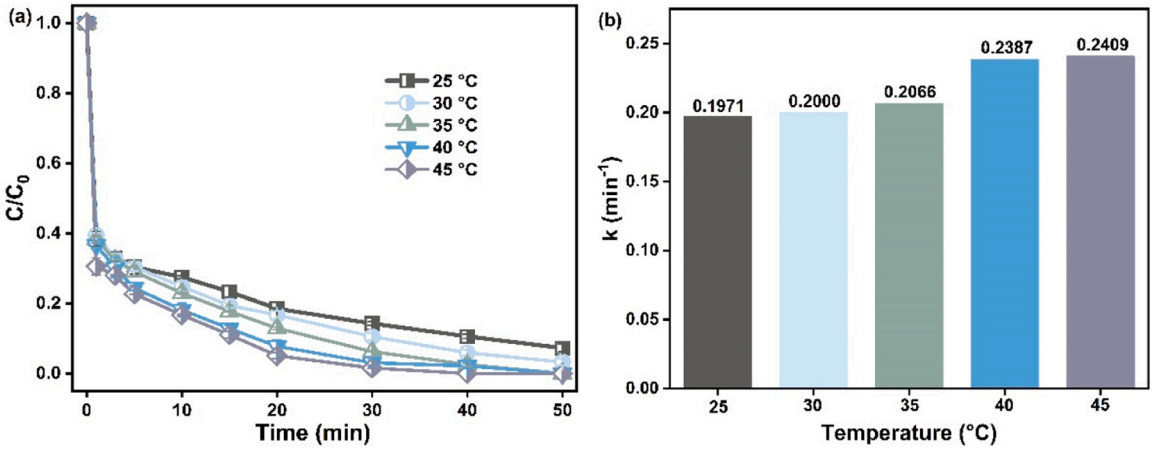

Fig. 6. (a) Effect of temperature on the degradation of RhB, (b) rate constant for different temperature. Reaction conditions: chalcopyrite 0.75 g/L, H_2O_2 43.0 mM, pH 5.1, and RhB 10 mg/L.

3.6. Effect of solution pH

The pH of the solution can significantly affect the Fenton system, influencing the stability of H_2O_2, the activity of the catalyst, the species of organic pollutant, and the oxidation potential of ·OH [36,48]. The homogeneous Fenton reaction is generally more efficient at acidic pH conditions, and Fenton-like process operated at neutral pH is imperative [53]. Fig. 7a shows the effect of initial pH (3.0, 4.0, 5.1, 7.0, 9.0, and 11.0) on the RhB degradation in the thermally activated chalcopyrite/H_2O_2 system. It can be seen that increasing pH causes the decline in RhB degradation. RhB degradation within 20 min is 97.7%, 98.2%, 83.3%, 71.1%, 40.1%, and 8.7% for pH 3.0, 4.0, 5.1, 7.0, 9.0, and 11.0, respectively. At an initial pH of 3.0, the degradation reaches 97.7% within 5 min, achieving a rapid degradation of RhB, which is consistent with the phenomenon of most Fenton reaction [9,14]. At neutral pH, complete degradation cannot be achieved at 50 min, but it may be obtained by extending the reaction time. As shown in Fig. 7b, the rate constant decreases from 0.6857 to 0.0142 min^{-1} when the pH increase from 3.0 to 11.0. Compared to the pyrite reported previously [45], thermally activated chalcopyrite has a wider reaction pH range.

Fig. S3 shows that solution pH rapidly decreases as the reaction proceeds, and this may be ascribed to the oxidation of S^{2-} in chalcopyrite (Eq. (3)) [74]. The oxidation of S^{2-} promotes Fe^{2+}/Fe^{3+} cycle and enhances H_2O_2 activation for the formation of hydroxyl radicals. Fig. S4 displays the final pH of the solution after the reaction, and the corresponding pH is 3.1, 3.8, 4.0, 4.5, 5.1, and 11.0, respectively. Fe^{2+} species in iron-bearing minerals are released more rapidly under acidic conditions than under alkaline conditions [2]. Chalcopyrite introduces dissolved iron and copper into solution and also increases the concentration of hydrogen ions lowering the pH of the solution [42]. At pH 3.0 and 4.0, metals in chalcopyrite are leached faster, favoring the generation of more ·OH for the degradation of RhB [25]. The decrease in RhB degradation at neutral pH may be due to the low leaching of metals as well as the precipitation of metal ions [7], which consume Fe^{2+} and Cu^{+} and inhibit the Fenton-like reactions, leading to a decrease in the RhB degradation. The alkaline condition is unfavorable for the generation of ·OH. Under alkaline conditions, H_2O_2 is transformed to less reactive species. In addition, S vacancies are created on the surface of chalcopyrite under acidic conditions, leading to the exposure of Cu and Fe active sites [55]. As a result, more Cu and Fe active sites can be released at low initial pH. This facilitates the activation of H_2O_2 and the degradation of RhB.

$$8Fe^{3+}+S^{2-}+4\ H_2O \rightarrow 8Fe^{2+}+SO_4^{2-}+8\ H^{+} \quad (3)$$

3.7. Effect of natural organic matter and anions

To further evaluate the feasibility for practical application of thermally activated chalcopyrite, the effect of co-existing substances such as natural organic matter and anions in wastewater is examined. Natural organic matter is a complex mixture of molecules, including humic

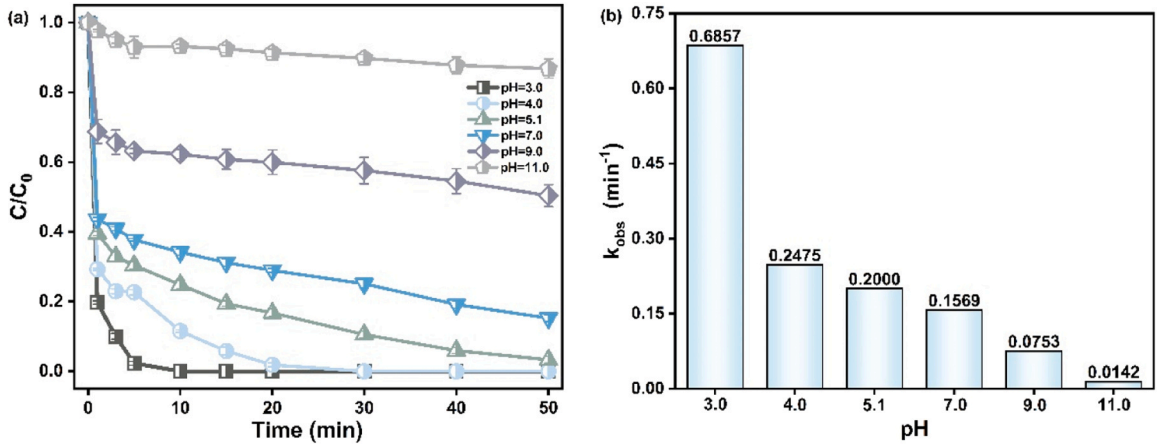

Fig. 7. (a) Effect of initial pH on the degradation of RhB, (b) rate constant for different initial pH. Reaction conditions: chalcopyrite 0.75 g/L, H_2O_2 43.0 mM, RhB 10 mg/L, and temperature 25 ℃.

acids, fulvic acids, and humus, and is present in large quantities in water sources [46]. Natural organic matter like humic acids can be harmful to aquatic organisms at high concentrations. Fig. 8a demonstrates that the degradation efficiency of RhB at 50 min decreases from 96.7% to 84.7% with increasing humic acid concentration from 0 mg/L to 20 mg/L. The negative effect of humic acid on RhB degradation can be ascribed to the competitive reactions with reactive oxygen species as well as adsorption onto catalyst surface. Humic acids could react rapidly with reactive radicals (10^4 L/(mg s)) [16]. Humic acids adsorb to the chalcopyrite surface, and competes with oxidants for surface active sites, inhibiting the activation process.

Fig. 8b represents the effect of Cl^- with different concentrations (0, 10, 20, 50 and 100 mM) on RhB degradation. The addition of chloride ions results in a slight decline in RhB degradation. Chloride ion can be a common radical scavenger in AOPs, as it can react with reactive radicals [64]. At high concentration, Cl^- reacts with more ·OH to produce the less oxidative chlorine radical (Cl·) (Eq. (4)) [30]. Fig. 8c shows RhB degradation in the presence of NO_3^-. The degradation of RhB is slightly inhibited with the addition of NO_3^-, decreasing from 96.73% to 78.48% with adding 100 mM of NO_3^-. This is attributed to the reaction of NO_3^- with ·OH (Eq. (5)), which forms redox NO_3··with lower potential (2.30 V) [4]. RhB degradation is nearly unchanged with the addition of SO_4^{2-} up to 100 mM (Fig. 8d). Overall, effective RhB degradation can be even under high-salt conditions, demonstrating the feasibility of thermally activated chalcopyrite for practical applications.

$$Cl^- + \cdot OH \rightarrow OH^- + Cl \quad (4)$$

$$NO_3^- + \cdot OH \rightarrow OH^- + NO_3\cdot \quad (5)$$

3.8. Identification of radical species

Degradation of organic pollutants by Fenton-like process highly depends on reactive ·OH [54]. Radical scavenging experiments are an effective strategy to reveal the role of different radicals in pollutant degradation. Isopropanol and tert-butanol can be used to scavenge ·OH (·OH in solution) and total ·OH (·OH in solution and ·OH adsorbed on catalyst surface), while p-benzoquinone is used to scavenge $\bullet O_2^-$ [19]. As shown in Fig. 9a, the degradation of RhB is significantly inhibited with the addition of tert-butanol and isopropanol. The little difference in RhB degradation after adding tert-butanol and isopropanol, the ·OH in solution plays a dominant role in Fenton-like degradation of RhB. The addition of p-benzoquinone also inhibits the degradation of RhB, indicating that $\bullet O_2^-$ contributes to RhB degradation. This is same to the results of Co-mediated removal of tetracycline using chalcopyrite [32].

To further identify the existence of radicals, EPR signals are determined using 5,5-Dietyl-1-pyrroline-N-oxide as the spin trapping agent. As shown in Fig. 9b, no distinct characteristic peaks are observed in the EPR spectrum before adding chalcopyrite (0 min). After reaction 5 min and 10 min, DMPO-·OH signals with an intensity ratio of 1:2:2:1 appear in the spectra ($a_N = a_H = 14.9$ g). The intensity of the signal peaks increases with the increase of reaction time as more ·OH is generated in the solution.

3.9. Catalytic mechanism

Thermal activation induces surface oxidation of natural chalcopyrite, and this promotes the leaching of Cu and Fe metal ions from chalcopyrite during the degradation of RhB. The change of Cu and Fe ions in solution during reaction is shown in Fig. S5. The leaching of Cu

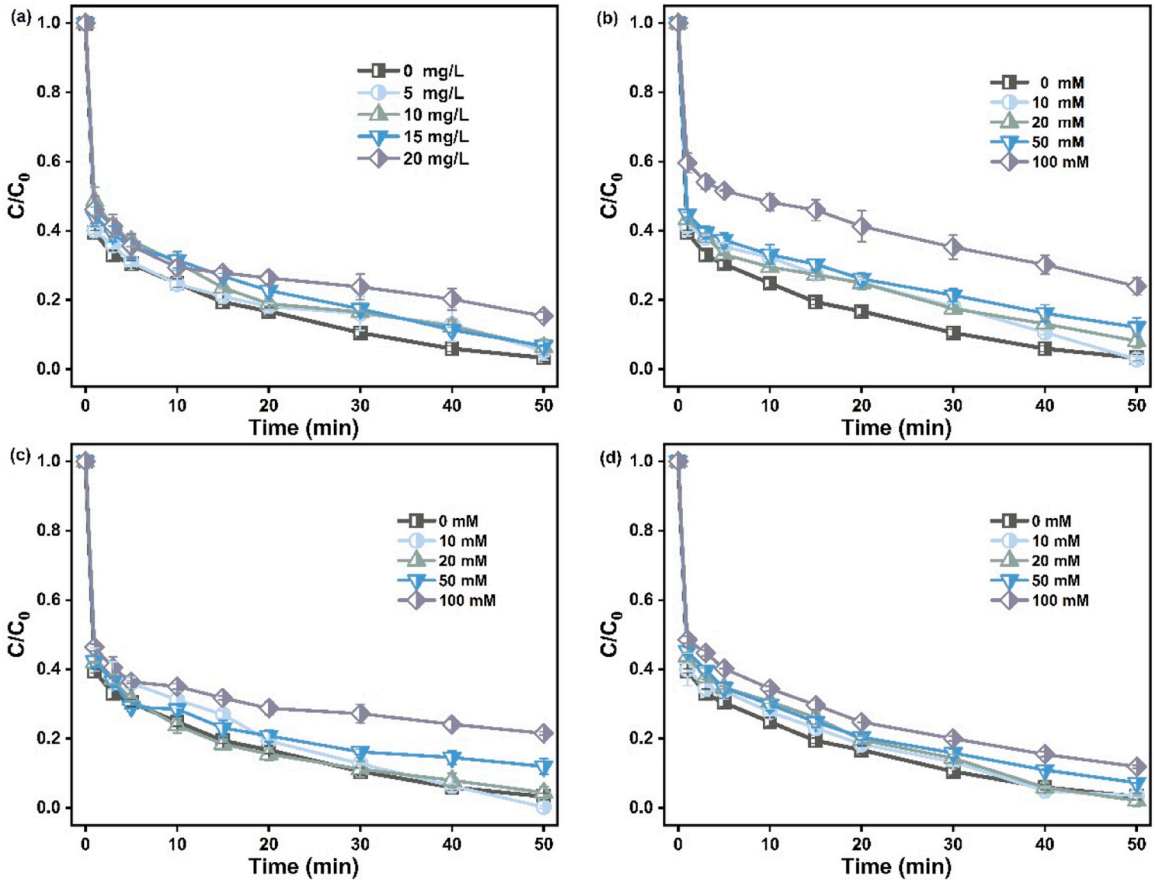

Fig. 8. Effect of natural organic matter and anions on the degradation of RhB: (a) humic acid, (b) Cl^-, (c) NO_3^-, and (d) SO_4^{2-}. Reaction conditions: chalcopyrite 0.75 g/L, H_2O_2 43.0 mM, pH 5.1, RhB 10 mg/L, and temperature 25 ℃.

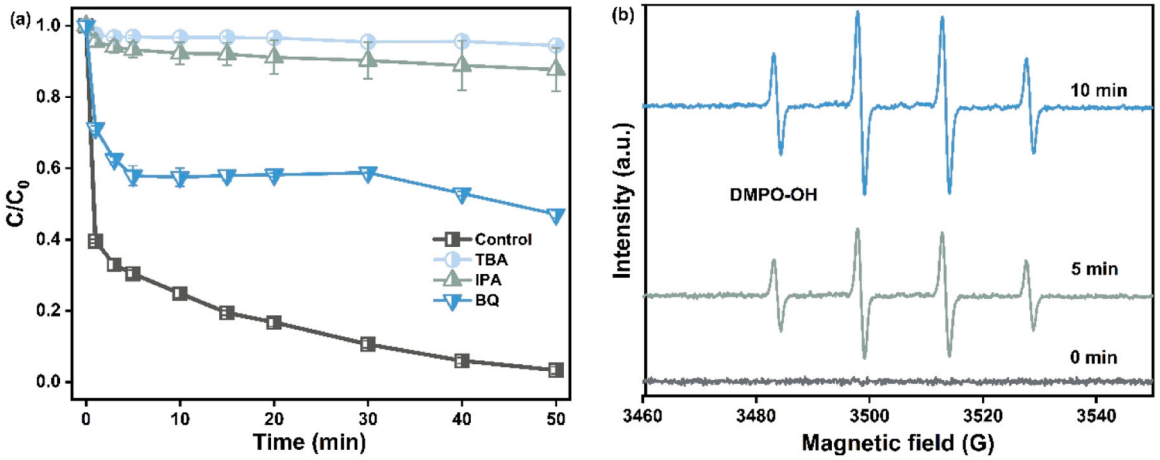

Fig. 9. (a) Effect of free radical trapping agents on the degradation of RhB, (b) EPR spectrum of·OH captured by 5,5-Dimethyl-1-pyrroline-N-oxide. Reaction conditions: chalcopyrite 0.75 g/L, H_2O_2 43.0 mM, pH 5.1, RhB 10 mg/L, temperature 25 ℃, isopropanol 10 mM, tert-butanol 10 mM, p-benzoquinone 5 mM.

and Fe ions from chalcopyrite can be observed, and the metal ions increase slightly with increasing reaction time. The metal leaching agrees with the poor reusability of the chalcopyrite catalyst in this catalytic system. Metal leaching can be attributed to the formation of dissolved sulfates on the surface of thermally activated chalcopyrite, and metals react rapidly with H_2O_2 to form ·OH. As the reaction proceeds, the concentration of Cu and Fe in the solution increases, which is responsible for the continuous leaching of metal ions from the catalyst. The degradation mechanism of RhB by thermally activated chalcopyrite can be shown in Fig. 10. The dissolution of surface sulphates from thermally activated chalcopyrite occurs first, and the metal ions in the solution can rapidly activate H_2O_2 to produce·OH, which is the main reason for effective RhB degradation. In addition, Cu^+ and Fe^{2+} species on the surface of chalcopyrite can also activate H_2O_2 to produce·OH accompanied by Cu^{2+}/Fe^{3+} via electron transfer reactions (Eq. (6)). Meanwhile, the sulphur atoms on the chalcopyrite surface can easily capture protons in solution and form sulphur vacancies, thus promoting the exposure of surface active sites [68]. The generated Cu^{2+} (E^{2+}_{Cu}=0.17 V) and Fe^{3+} (E^{2+}_{Fe} = 0.77 V) can be reduced by sulfur species such as S^{2-} (E^{0}_{SS}=−0.508 V) and S_2^{2-} (E^{2-}_{SS}=−0.48 V) (Eqs. (7)–(9)). Fe^{2+} can be regenerated by the interaction between Cu^+ and Fe^{3+} (Eq. (10)). The Cu^+ and Fe^{2+} species regenerated on the chalcopyrite surface can again activate H_2O_2 and continue to produce reactive radicals for RhB degradation.

$$Cu^+/Fe^{2+}+H_2O_2 \rightarrow Cu^{2+}/Fe^{3+}+\bullet OH+OH^- \quad (6)$$

$$S^{2-}+Cu^{2+}/Fe^{3+} \rightarrow Cu^+/Fe^{2+}+S_2^{2-} \quad (7)$$

$$S_2^{2-}+Cu^{2+}/Fe^{3+} \rightarrow Cu^+/Fe^{2+}+ S_n^{2-} \quad (8)$$

$$S_n^{2-}+Cu^{2+}/Fe^{3+} \rightarrow Cu^+/Fe^{2+}+SO_4^{2-} \quad (9)$$

$$Cu^+ + Fe^{3+} \rightarrow Fe^{2+} + Cu^{2+} \quad (10)$$

4. Conclusions

In this work, thermal activation is proposed to improve the catalytic activity of natural chalcopyrite. The physicochemical properties of the thermally activated chalcopyrite are characterized by multiple techniques. The RhB degradation reaches 96.7% at 50 min under the conditions of H_2O_2 concentration 43.0 mM, chalcopyrite 0.75 g/L, initial pH 4.0, and reaction temperature 25 ℃. RhB degradation can be obtained under broad pH and exhibits high resistance to natural organic matter and anions. The activation energy for RhB degradation in the catalytic system is 9 kJ/mol. The radical scavenging experiments and EPR techniques prove the dominant role of hydroxyl groups in RhB degradation. Sulphates on the surface of thermally activated chalcopyrite readily produce metal ions and activate H_2O_2 to produce hydroxyl radicals through Fenton-like reactions. The Cu^+ and Fe^{2+} species on the

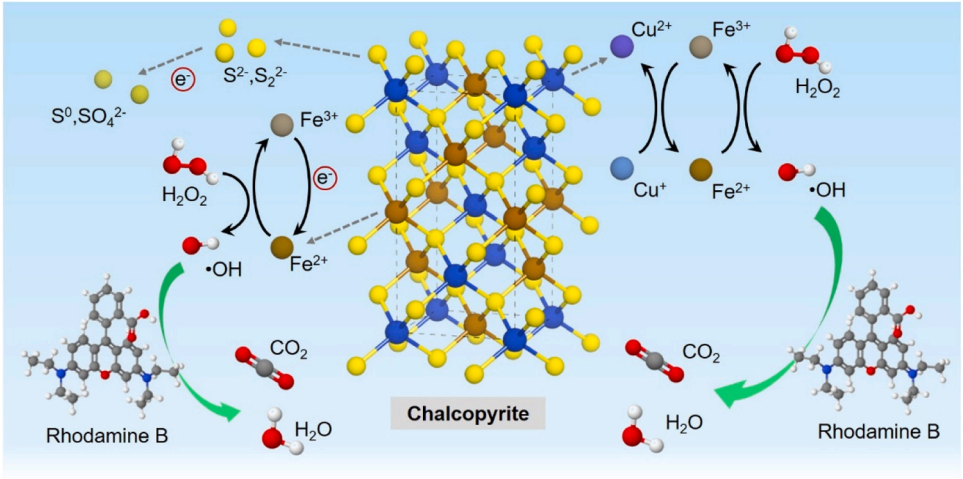

Fig. 10. The mechanism of RhB degradation in thermally activated chalcopyrite/H_2O_2 system.

surface of chalcopyrite can activate H_2O_2 to generate ·OH accompanied by Cu^{2+}/Fe^{3+} through electron transfer reactions. This study preliminarily reveals the mechanism of thermal activation to improve the activity of natural chalcopyrite, and provides a theoretical basis for enhancing the efficient degradation of organic pollutants by natural minerals. It is clear that proposed method of chalcopyrite activation is possible and easy to implement in industrial practice. Further studies should be conducted to improve the stability and reusability of the chalcopyrite catalyst, as well as the catalytic degradation of emerging organic pollutants in wastewater.

CRediT authorship contribution statement

Jiapeng Yang led the experimental studies and writing of the manuscript, and contributed to research design and analysis of results; Shaoyong Lu, Yijun Cao, and Grzegorz Boczkaj contributed to analysis of results and revision of the manuscript; Kai Jia and Chongqing Wang contributed to the research design, analysis of results and writing of the manuscript.

Declaration of Competing Interest

The authors declare that they have no known competing financial interests or personal relationships that could have appeared to influence the work reported in this paper.

Data availability

Data will be made available on request.

Acknowledgements

This work was supported by the National Natural Science Foundation of China (No. 52004251), the Open Foundation of State Key Laboratory of Mineral Processing (No. BGRIMM-KJSKL-2020–08), and the Project of Zhongyuan Critical Metals Laboratory of Zhengzhou University.

Appendix A. Supporting information

Supplementary data associated with this article can be found in the online version at doi:10.1016/j.jece.2023.111469.

References

[1] A. Asghar, A.A. Abdul Raman, W.M.A. Wan Daud, Advanced oxidation processes for in-situ production of hydrogen peroxide/hydroxyl radical for textile wastewater treatment: a review, J. Clean. Prod. 87 (2015) 826–838.
[2] S. Bae, D. Kim, W. Lee, Degradation of diclofenac by pyrite catalyzed Fenton oxidation, Appl. Catal. B: Environ. 134–135 (2013) 93–102.
[3] B. Bethi, G.B. Radhika, L.M. Thang, et al., Photocatalytic decolourization of Rhodamine-B dye by visible light active ZIF-8/BiFeO3 composite, Environ. Sci. Pollut. Res. 30 (10) (2023) 25532–25545.
[4] A.M. Bergquist, J.K. Choe, T.J. Strathmann, et al., Evaluation of a hybrid ion exchange-catalyst treatment technology for nitrate removal from drinking water, Water Res. 96 (2016) 177–187.
[5] E. Brillas, S. Garcia-Segura, Benchmarking recent advances and innovative technology approaches of Fenton, photo-Fenton, electro-Fenton, and related processes: A review on the relevance of phenol as model molecule, Sep. Purif. Technol. 237 (2020), 116337.
[6] G. Boczkaj, A. Fernandes, Wastewater treatment by means of advanced oxidation processes at basic pH conditions: A review, Chem. Eng. J. 320 (2017) 608–633.
[7] H. Che, S. Bae, W. Lee, Degradation of trichloroethylene by Fenton reaction in pyrite suspension, J. Hazard. Mater. 185 (2) (2011) 1355–1361.
[8] S. Chen, D. Du, Degradation of n-butyl xanthate using fly ash as heterogeneous Fenton-like catalyst, J. Cent. South Univ. 21 (4) (2014) 1448–1452.
[9] H. Chen, Z. Zhang, Z. Yang, et al., Heterogeneous fenton-like catalytic degradation of 2,4-dichlorophenoxyacetic acid in water with FeS, Chem. Eng. J. 273 (2015) 481–489.
[10] G.R. Da Silva, E.R.L. Espiritu, S. Mohammadi-Jam, et al., Surface characterization of microwave-treated chalcopyrite, Colloids Surf. A: Physicochem. Eng. Asp. 555 (2018) 407–417.
[11] G.R. Da Silva, K.E. Waters, The effects of microwave irradiation on the floatability of chalcopyrite, pentlandite and pyrrhotite, Adv. Powder Technol. 29 (12) (2018) 3049–3061.
[12] Y. Deng, X. Zhao, J. Luo, et al., Magnetic recyclable CoFe2O4@PPy prepared by in situ Fenton oxidization polymerization with advanced photo-Fenton performance, RSC Adv. 10 (4) (2020) 1858–1869.
[13] Z.-H. Diao, J.-J. Liu, Y.-X. Hu, et al., Comparative study of Rhodamine B degradation by the systems pyrite/H_2O_2 and pyrite/persulfate: Reactivity, stability, products and mechanism, Sep. Purif. Technol. 184 (2017) 374–383.
[14] Z. Diao, X. Xu, D. Jiang, et al., Enhanced catalytic degradation of ciprofloxacin with FeS_2/SiO_2 microspheres as heterogeneous Fenton catalyst: Kinetics, reaction pathways and mechanism, J. Hazard. Mater. 327 (2017) 108–115.
[15] C. Droguett, R. Salazar, E. Brillas, et al., Treatment of antibiotic cephalexin by heterogeneous electrochemical Fenton-based processes using chalcopyrite as sustainable catalyst, Sci. Total Environ. 740 (2020), 140154.
[16] J. Dong, W. Xu, S. Liu, et al., Lignin-derived biochar to support $CoFe_2O_4$: Effective activation of peracetic acid for sulfamethoxazole degradation, Chem. Eng. J. 430 (2022), 132868.
[17] N. Faris, R. Ram, M. Chen, et al., The effect of thermal pre-treatment on the dissolution of chalcopyrite ($CuFeS_2$) in sulfuric acid media, Hydrometallurgy 169 (2017) 68–78.
[18] K. Fedorov, K. Dinesh, X. Sun, et al., Synergistic effects of hybrid advanced oxidation processes (AOPs) based on hydrodynamic cavitation phenomenon – A review, Chem. Eng. J. 432 (2022), 134191.
[19] K. Fedorov, M.P. Rayaroth, N.S. Shah, et al., Activated sodium percarbonate-ozone (SPC/O_3) hybrid hydrodynamic cavitation system for advanced oxidation processes (AOPs) of 1,4-dioxane in water, Chem. Eng. J. 456 (2023), 141027.
[20] Q. Guo, W. Zhu, D. Yang, et al., A green solar photo-Fenton process for the degradation of carbamazepine using natural pyrite and organic acid with in-situ generated H_2O_2, Sci. Total Environ. 784 (2021), 147187.
[21] T. Hirajima, M. Mori, O. Ichikawa, et al., Selective flotation of chalcopyrite and molybdenite with plasma pre-treatment, Miner. Eng. 66–68 (2014) 102–111.
[22] T. Hirajima, H. Miki, G.P.W. Suyantara, et al., Selective flotation of chalcopyrite and molybdenite with H_2O_2 oxidation, Miner. Eng. 100 (2017) 83–92.
[23] X. Hou, X. Huang, F. Jia, et al., Hydroxylamine Promoted Goethite Surface Fenton Degradation of Organic Pollutants, Environ. Sci. Technol. (2017) 5118–5126, 51 9.
[24] F. Ji, C. Li, X. Wei, et al., Efficient performance of porous Fe_2O_3 in heterogeneous activation of peroxymonosulfate for decolorization of Rhodamine B, Chem. Eng. J. 231 (2013) 434–440.
[25] C. Kantar, Role of low molecular weight organic acids on pyrite dissolution in aqueous systems: implications for catalytic chromium (VI) treatment, Water Sci. Technol. 74 (1) (2016) 99–109.
[26] T.K. Kasonga, M.A. Coetzee, I. Kamika, et al., Endocrine-disruptive chemicals as contaminants of emerging concern in wastewater and surface water: A review, J. Environ. Manag. 277 (2021), 111485.
[27] L. Lai, Y. He, H. Zhou, et al., Critical review of natural iron-based minerals used as heterogeneous catalysts in peroxide activation processes: Characteristics, applications and mechanisms, J. Hazard. Mater. 416 (2021), 125809.
[28] X. Li, K. Cui, Z. Guo, et al., Heterogeneous Fenton-like degradation of tetracyclines using porous magnetic chitosan microspheres as an efficient catalyst compared with two preparation methods, Chem. Eng. J. 379 (2020), 122324.
[29] Y. Li, H. Dong, L. Li, et al., Efficient degradation of sulfamethazine via activation of percarbonate by chalcopyrite, Water Res. 202 (2021), 117451.
[30] Y. Li, H. Dong, L. Li, et al., Recent advances in waste water treatment through transition metal sulfides-based advanced oxidation processes, Water Res. 192 (2021), 116850.
[31] N. Li, X. He, J. Ye, et al., H_2O_2 activation and contaminants removal in heterogeneous Fenton-like systems, J. Hazard. Mater. 458 (2023), 131926.
[32] J. Li, D. Zhong, J. Huang, et al., Cobalt mediated perovskite as efficient Fenton-like catalysts for the tetracycline removal over a neutral condition: The importance of superoxide radical, Chemosphere 313 (2023), 137564.
[33] W. Li, Y. Li, Z. Wang, et al., Selective flotation of chalcopyrite from pyrite via seawater oxidation pretreatment, Int. J. Min. Sci. Technol. (2023).
[34] Y. Liu, W. Jin, Y. Zhao, et al., Enhanced catalytic degradation of methylene blue by α-Fe_2O_3/graphene oxide via heterogeneous photo-Fenton reactions, Appl. Catal. B: Environ. 206 (2017) 642–652.
[35] C. Liu, W. Cai, M. Zhai, et al., Decoupling of wastewater eco-environmental damage and China's economic development, Sci. Total Environ. 789 (2021), 147980.
[36] K. Liu, F. Zheng, Y. Xiao, et al., High Fe utilization efficiency and low toxicity of $Fe_3C@Fe^0$ loaded biochar for removing of tetracycline hydrochloride in wastewater, J. Clean. Prod. 353 (2022), 131630.
[37] G. Liu, X. Zhang, H. Liu, et al., Biochar/layered double hydroxides composites as catalysts for treatment of organic wastewater by advanced oxidation processes: A review, Environ. Res. 234 (2023), 116534.
[38] H. Liu, X. Li, X. Zhang, et al., Harnessing the power of natural minerals: A comprehensive review of their application as heterogeneous catalysts in advanced oxidation processes for organic pollutant degradation, Chemosphere 337 (2023), 139404.
[39] Q. Luo, Q. Shi, D. Liu, et al., Effect of deep oxidation of chalcopyrite on surface properties and flotation performance, Int. J. Min. Sci. Technol. 32 (4) (2022) 907–914.
[40] A.V. Mohod, M. Momotko, N.S. Shah, et al., Degradation of Rhodamine dyes by Advanced Oxidation Processes (AOPs)–Focus on caviatation and photocatalysis-A critical review, Water Resour. Ind. (2023), 100220.

[41] A. Nawaz, M. Atif, A. Khan, et al., Solar light driven degradation of textile dye contaminants for wastewater treatment–studies of novel polycationic selenide photocatalyst and process optimization by response surface methodology desirability factor, Chemosphere 328 (2023), 138476.
[42] X. Nie, G. Li, S. Li, et al., Highly efficient adsorption and catalytic degradation of ciprofloxacin by a novel heterogeneous Fenton catalyst of hexapod-like pyrite nanosheets mineral clusters, Appl. Catal. B: Environ. 300 (2022), 120734.
[43] J. Peng, H. Zhou, W. Liu, et al., Insights into heterogeneous catalytic activation of peroxymonosulfate by natural chalcopyrite: pH-dependent radical generation, degradation pathway and mechanism, Chem. Eng. J. 397 (2020), 125387.
[44] P. Rupa Ranjani, P.M. Anjana, R.B. Rakhi, Solvothermal synthesis of $CuFeS_2$ nanoflakes as a promising electrode material for supercapacitors, J. Energy Storage 33 (2021), 102063.
[45] F. Sang, Z. Yin, W. Wang, et al., Degradation of ciprofloxacin using heterogeneous Fenton catalysts derived from natural pyrite and rice straw biochar, J. Clean. Prod. 378 (2022), 134459.
[46] A. Shan, U. Farooq, S. Lyu, et al., Efficient removal of trichloroethylene in surfactant amended solution by nano Fe^0-Nickel bimetallic composite activated sodium persulfate process, Chem. Eng. J. 386 (2020), 123995.
[47] F. Sun, H. Liu, H. Wang, et al., A novel discovery of a heterogeneous Fenton-like system based on natural siderite: A wide range of pH values from 3 to 9, Sci. Total Environ. 698 (2020), 134293.
[48] R. Sun, X. Zhang, C. Wang, et al., Co-carbonization of red mud and waste sawdust for functional application as Fenton catalyst: Evaluation of catalytic activity and mechanism, J. Environ. Chem. Eng. 9 (4) (2021), 105368.
[49] X. Tang, Y. Chen, K. Liu, et al., Selective flotation separation of molybdenite and chalcopyrite by thermal pretreatment under air atmosphere, Colloids Surf. A: Physicochem. Eng. Asp. 583 (2019), 123958.
[50] N. Thomas, D.D. Dionysiou, S.C. Pillai, Heterogeneous Fenton catalysts: A review of recent advances, J. Hazard. Mater. 404 (2021), 124082.
[51] C. Wang, Y. Cao, H. Wang, Copper-based catalyst from waste printed circuit boards for effective Fenton-like discoloration of Rhodamine B at neutral pH, Chemosphere 230 (2019) 278–285.
[52] H. Wang, T. Chen, D. Chen, et al., Sulfurized oolitic hematite as a heterogeneous Fenton-like catalyst for tetracycline antibiotic degradation, Appl. Catal. B: Environ. 260 (2020), 118203.
[53] C. Wang, R. Huang, R. Sun, Green one-spot synthesis of hydrochar supported zero-valent iron for heterogeneous Fenton-like discoloration of dyes at neutral pH, J. Mol. Liq. 320 (2020), 114421.
[54] C. Wang, R. Sun, R. Huang, et al., A novel strategy for enhancing heterogeneous Fenton degradation of dye wastewater using natural pyrite: Kinetics and mechanism, Chemosphere 272 (2021), 129883.
[55] J. Wang, Z. Wang, Y. Cheng, et al., Molybdenum disulfide (MoS_2): A novel activator of peracetic acid for the degradation of sulfonamide antibiotics, Water Res. 201 (2021), 117291.
[56] C. Wang, R. Sun, R. Huang, Highly dispersed iron-doped biochar derived from sawdust for Fenton-like degradation of toxic dyes, J. Clean. Prod. 297 (2021), 126681.
[57] L. Wang, D. Luo, J. Yang, et al., Metal-organic frameworks-derived catalysts for contaminant degradation in persulfate-based advanced oxidation processes, J. Clean. Prod. 375 (2022), 134118.
[58] C. Wang, R. Huang, R. Sun, et al., Microplastics separation and subsequent carbonization: Synthesis, characterization, and catalytic performance of iron/carbon nanocomposite, J. Clean. Prod. 330 (2022), 129901.
[59] C. Wang, J. Yang, R. Huang, et al., Mechanical activation of natural chalcopyrite for improving heterogeneous Fenton degradation of tetracycline, J. Cent. South Univ. 29 (12) (2022) 3884–3895.
[60] J. Wang, Q. Zhang, J. Peng, et al., Persulfate activation by copper tailings with hydroxylamine: efficiency, mechanism and DFT calculations, Sep. Purif. Technol. 297 (2022), 121472.
[61] L. Wang, D. Luo, O. Hamdaoui, et al., Bibliometric analysis and literature review of ultrasound-assisted degradation of organic pollutants, Sci. Total Environ. 876 (2023), 162551.
[62] M. Xia, M. Long, Y. Yang, et al., A highly active bimetallic oxides catalyst supported on Al-containing MCM-41 for Fenton oxidation of phenol solution, Appl. Catal. B: Environ. 110 (2011) 118–125.
[63] S. Xin, G. Liu, X. Ma, et al., High efficiency heterogeneous Fenton-like catalyst biochar modified $CuFeO_2$ for the degradation of tetracycline: Economical synthesis, catalytic performance and mechanism, Appl. Catal. B: Environ. 280 (2021), 119386.
[64] D. Xing, S. Shao, Y. Yang, et al., Mechanistic insights into the efficient activation of peracetic acid by pyrite for the tetracycline abatement, Water Res. 222 (2022), 118930.
[65] H. Xu, D. Wang, J. Ma, et al., A superior active and stable spinel sulfide for catalytic peroxymonosulfate oxidation of bisphenol S, Appl. Catal. B: Environ. 238 (2018) 557–567.
[66] W. Xu, R. Zou, B. Jin, et al., The ins and outs of pharmaceutical wastewater treatment by microbial electrochemical technologies, Sustain. Horiz. 1 (2022), 100003.
[67] J. Yang, R. Huang, Y. Cao, et al., Heterogeneous Fenton degradation of persistent organic pollutants using natural chalcopyrite: effect of water matrix and catalytic mechanism, Environ. Sci. Pollut. Res. 29 (50) (2022) 75651–75663.
[68] K. Yang, Z. Zhai, H. Liu, et al., Peracetic acid activation by natural chalcopyrite for metronidazole degradation: Unveiling the effects of Cu-Fe bimetallic sites and sulfur species, Sep. Purif. Technol. 305 (2023), 122500.
[69] E.N. Zare, A. Motahari, M. Sillanpää, Nanoadsorbents based on conducting polymer nanocomposites with main focus on polyaniline and its derivatives for removal of heavy metal ions/dyes: A review, Environ. Res. 162 (2018) 173–195.
[70] M. Zhang, Q.X. Yao, W. Guan, et al., Layered double hydroxide-supported carbon dots as an efficient heterogeneous fenton-like catalyst for generation of hydroxyl radicals, J. Phys. Chem. C. 118 (2014) 10441–10447.
[71] Y. Zhang, T. Chen, Y. Zhao, et al., Catalytic effect of siderite on H_2O_2 oxidation of carmine dye: Performance, mechanism and kinetics, Appl. Geochem. 106 (2019) 26–33.
[72] Q. Zhang, D. Zheng, B. Bai, et al., Solar-driven photothermal-Fenton removal of ofloxacin through waste natural pyrite with dual-function, Colloids Surf. A: Physicochem. Eng. Asp. 641 (2022), 128574.
[73] X. Zhang, H. Sun, Y. Shi, et al., Oxalated zero valent iron enables highly efficient heterogeneous Fenton reaction by self-adapting pH and accelerating proton cycle, Water Res. 235 (2023), 119828.
[74] L. Zhao, Y. Chen, Y. Liu, et al., Enhanced degradation of chloramphenicol at alkaline conditions by S(-II) assisted heterogeneous Fenton-like reactions using pyrite, Chemosphere 188 (2017) 557–566.
[75] R. Zheng, J. Li, R. Zhu, et al., Enhanced Cr(VI) reduction on natural chalcopyrite mineral modulated by degradation intermediates of RhB, J. Hazard. Mater. 423 (2022), 127206.
[76] L. Zeng, J. Gong, J. Dan, et al., Novel visible light enhanced Pyrite-Fenton system toward ultrarapid oxidation of p-nitrophenol: Catalytic activity, characterization and mechanism, Chemosphere 228 (2019) 232–240.
[77] M. Zouheir, K. Tanji, J.A. Navio, et al., Effective photocatalytic conversion of formic acid using iron, copper and sulphate doped TiO_2, J. Cent. South Univ. 29 (11) (2022) 3592–3607.